Compact series elastic actuator for a wrist exoskeleton for daily living assistance

Compact Series Elastic Actuator for a Wrist Exoskeleton for Daily Living Assistance

Andrea Botta [0000-0002-7272-7132] [1], Luigi Tagliavini[1], Giovanni Colucci [1], Lorenzo Baglieri[1], Simone Duretto[1], Yukio Takeda[2], and Giuseppe Quaglia[1]

[1] Politecnico di Torino
DIMEAS - Department of Mechanical and Aerospace Engineering
{andrea.botta, luigi.tagliavini, giovanni_colucci, lorenzo.baglieri, simone.duretto,giuseppe.quaglia}@polito.it
[2] Tokyo Institute of Technology
Department of Mechanical Engineering
takeda.y.aa@m.titech.ac.jp

Abstract This study presents the preliminary design of a compact compliant actuator for assisting wrist motions or similar joints within exoskeleton applications. Leveraging additive manufacturing techniques, a lightweight design approach is pursued, with most components fabricated from nylon. The actuator features a 2-stage cycloidal transmission and tendon-like transmission, optimized for space efficiency. Dynamic modeling drives the design process, culminating in a proposed final actuator design. Fabrication of a prototype is planned for assessment against modeled dynamics, with integration into an exoskeleton contingent upon promising results. Future design iterations will focus on the elastic element, exploring custom torsion spring design or commercial spring options to achieve the desired stiffness.

Keywords: Series Elastic Actuator; Bowden cable; Wrist Exoskeleton; SDG3; Daily Living Assistance; Rehabilitation; Disability

1 Introduction

As of 2021, about 16% of the global population experiences some form of disability, with 2-4% facing significant challenges in daily activities [1]. As the population ages, there is a concurrent increase in the demand for assistive devices. Notably, devices aiding upper limb functions are highly sought-after due to their facilitation of essential daily tasks [2], thereby fostering user independence and inclusivity [1].

Given these premises, the development of assistive robotic devices is on the rise, encompassing both the exoskeleton and the end-effector types [3-5]. Gonçalves et al. designed a desk-based end-effector robot that can achieve two distinct wrist motions through setup adjustments [6]. Shi et al. presented a cable-driven 3-DOF robot [7]. This wearable robot is non-portable due to a bulky actuation sub-system fixed to the ground.

However, the literature reveals a shortage of lightweight, wearable and compact solutions targeting assistance for the wrist joint. To address this issue, the authors

previously proposed a wearable cable-driven solution for wrist joint rehabilitation [8,9]. While promising, this proposal was found to be too bulky to be effective as a daily task assistive device. In this study, we introduce a novel concept for a robotic device aimed at assisting with daily tasks, with a particular emphasis on its actuation subsystem. This new approach seeks to address the shortcomings of previous designs and offer a more practical solution for supporting wrist joint functionality in everyday activities.

2 Wrist exoskeleton actuator design

2.1 Requirements and concept design

The proposed exoskeleton aims for maximum acceptance through a lightweight and compact design. To achieve this, employing a remote actuation using Bowden cables presents a promising solution to reduce the load and encumbrance near the wrist, with potential placement options including the upper arm or even the back (Fig.1a).

The kinematic chain of the exoskeleton seeks to emulate the human wrist. Despite its complexity, it is usually simplified as a universal joint with perpendicular but non-intersecting axes (Fig.1b). These axes correspond to the two wrist motions: radial/ulnar deviation (RUD) (Fig.1c) and the flexion/extension (FE) (Fig.1d). Each degree of freedom (DOF) operates independently, necessitating its actuator system. The actuator transmission ends with a tendon-like architecture, driven by a pair of Bowden cables for remote actuation and improved weight distribution. The FE cables pair moves the revolute joint A via a pulley, rotating link AB and consequently the whole hand. Similarly, RUD cables actuate the pulley at joint B. Joint A is fixed by means of a bracelet to the forearm, while joint B moves in response to FE motion.

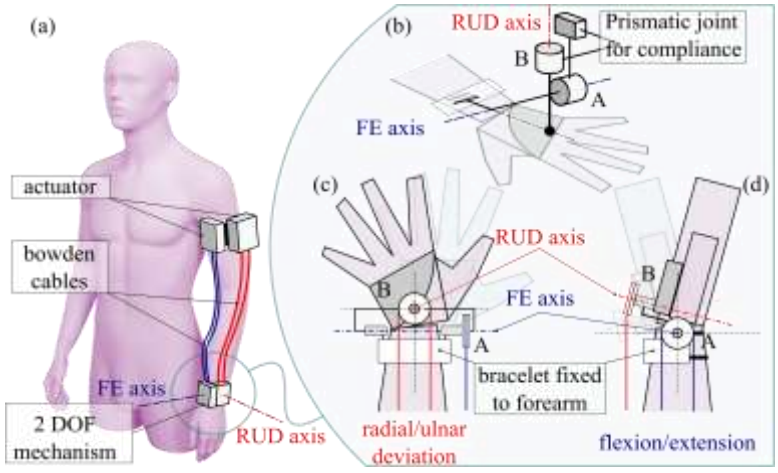

Fig. 1. Wrist exoskeleton concept. (**a**) Overall concept of the exoskeleton. (**b**) Functional diagram of the 2 DOF mechanism. (**c**) Radial/ulnar deviation (RUD) motion. (**d**) Flexion/extension (FE) motion.

Both motions exhibit different range of motions, namely $(-71°, +73°)$ for FE and $(-33°, +19°)$ for RUD [10], yet share similar maximum torque and angular velocity requirements, about 8 Nm and 12 rad/s respectively [6, 11]. Therefore, a single actuation sub-system can be designed with a symmetrical range of motion of $\pm 80°$ to work for both motions and both hands.

A crucial requirement is precise and responsive torque control to effectively assist wrist motions. To achieve this, an elastic element is integrated between the actuator transmission and the hand at joints A and B, creating a Series Elastic Actuator (SEA) architecture. This addition introduces compliance between the hand and the exoskeleton while simplifying torque control into displacement control of the elastic element. Furthermore, a SEA architecture mitigates issues related to Bowden cables bending, which can affect the efficiency of the transmission. Compared to rigid transmission, SEAs have a reduced bandwidth, nevertheless wrist motions are slow and with a maximum bandwidth of 8-12 Hz [12], hence this limitation is not critical.

2.2 Functional design

Figure 2 illustrates a diagram of the actuation system, divided into its two main elements based on their location. Positioned on the upper arm, an electric motor, coupled with a dedicated gearbox, drives a pulley controlling the Bowden cables pair. These cables, in turn, actuate a second pulley, governing one of the two axes of the 2 DOF exoskeleton described before. To obtain a proper SEA, a torsional elastic element with stiffness k_s is placed between the latter pulley and the corresponding exoskeleton joint. Its displacement can be directly measured by a single sensor, or two different sensors could be used to measure the absolute rotation of each ends of the elastic element.

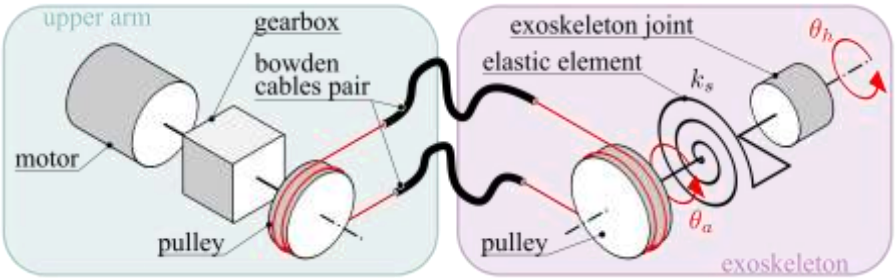

Fig. 2. Functional diagram of the actuator system divided into its two main subsystems based on their location.

Both hand motions require relatively high maximum torque and low maximum angular speed. Consequently, conventional electric motors need a transmission with a significant transmission ratio. Considering constraints such as size and weight, the development of the transmission starting from a 2-stages cycloidal drive proved to be advantageous. Two additional pulley systems (one being the tendon-like system) facilitate achieving the required transmission ratio. A diagram of the entire transmission is shown in Fig.3a.

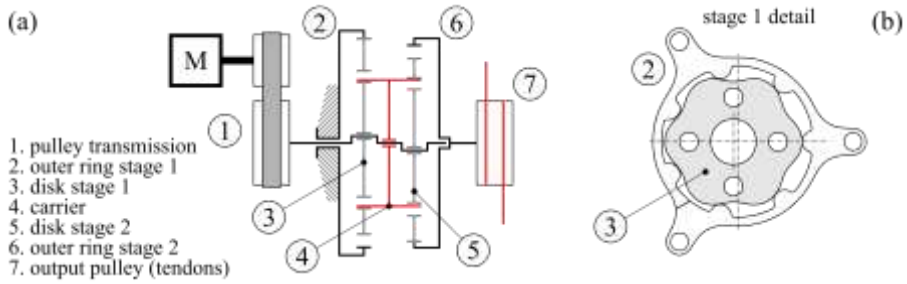

Fig. 3. (**a**) Functional diagram of the actuator transmission with its elements. (**b**) Detail of the first stage of the cycloidal drive.

Compared to a single-stage cycloidal drive, the proposed two-stage design effectively balances the eccentric disk with a second stage and reduces the number of lobes in the outer rings and disks. This configuration allows for larger and more durable lobes.

To maximize the cycloidal drive transmission ratio, the following constraints are set

$$\begin{aligned} z_1 &= z_2 + 1 \\ z_3 &= z_4 + 1 \\ z_4 &= z_2 - 1 \end{aligned} \tag{1}$$

where z_1, z_2, z_3, z_4 are the number of lobes of the first outer ring, the first disk, the second outer ring, and the second disk, respectively. With this configuration, the cycloidal drive transmission ratio is

$$\tau_{cyl} = \frac{\omega_{out}}{\omega_{in}} = \frac{1}{z_2^2} \tag{2}$$

Considering the T-Motor GL30 brushless motor, the parameters in Table 1 are used to achieve the desired performance.

Table 1. Transmission parameters

Parameter	*Value*	*Parameter*	*Value*
Motor rated speed	2200 rpm	Cycloidal outer diameter	34 mm
Motor rated torque	0.08 Nm	Fixed lobes diameter	5 mm
Motor rated power	18.5 W	Carrier pins diameter	2 mm
Motor stall torque	0.28 Nm	Cycloidal output pulley diameter	38 mm
Motor diameter	34.5 mm	Wrist joint pulley diameter	40 mm
Motor pulley diameter	38 mm	Motor pulley transmission ratio	1:1.13
Cycloidal input pulley diameter	43 mm	Cycloidal transmission ratio	1:36
Cycloidal Disk stage 1 lobes z_2	6	Tendon transmission ratio	1:1.05
Cycloidal eccentricity	1 mm	Total transmission ratio	1:42.7

2.3 Sizing of the elastic element

The SEA elastic element design aims to maximize the actuator bandwidth (high stiffness) while minimizing output mechanical impedance (low stiffness). To do so, the system represented in the block diagram shown in Fig.4 can be defined. The actuator, as described earlier, applies a torque τ_a to rotate the pulley integral to the exoskeleton joint (with inertia J_a and friction β_a) by an angle θ_a. This pulley is connected to the hand (inertia J_h) through an elastic element with stiffness k_s, resulting in a hand motion θ_h. To effectively control τ_a, the spring displacement $\theta_s = \theta_a - \theta_h$ is measured and utilized to estimate the torque applied to the hand τ_h. Subsequently, a simple PD control (K_P proportional gain, K_D derivative gain) generates the proper actuation torque τ_r. Such reference value is generated by a higher-level controller to achieve the desired assistance and or transparency of the device.

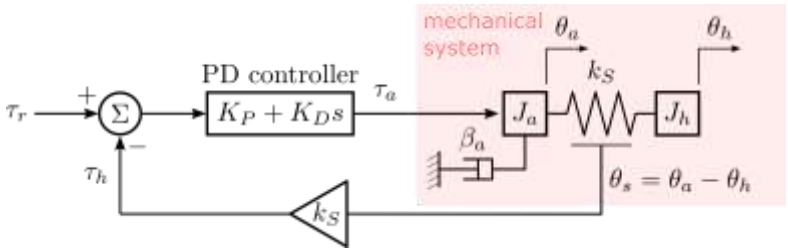

Fig. 4. Block diagram of the series elastic actuator. Angular motion is represented as linear for ease of representation.

The system behavior can is characterized by its transfer functions, including the open-loop transfer function

$$G_{OL}(s) = \frac{\tau_h}{\tau_a} = \frac{1}{\frac{J_a}{k_s}s^2 + \frac{\beta_a}{k_s}s + 1} \tag{3}$$

the closed-loop transfer function

$$G_{CL}(s) = \frac{\tau_h}{\tau_r} = \frac{K_D\, s + K_P}{\frac{J_a}{k_s}s^2 + \frac{\beta_a + K_D k_s}{k_s}s + K_P + 1} \tag{4}$$

and the output impedance transfer function

$$Z(s) = \frac{\tau_h}{\theta_h} = -\frac{J_a\, s^2 + \beta_a\, s}{\frac{J_a}{k_s}s^2 + \frac{\beta_a + K_D k_s}{k_s}s + K_P + 1} \tag{5}$$

It's noteworthy that this analysis assumes the actuator operates without a load ($J_h = 0$), as commonly done.

After an iterative design process, a compromise between bandwidth and impedance led to selecting a stiffness value of $k_s = 23$ Nm/rad was chosen. The corresponding frequency responses are represented in Fig.5. The $G_{OL}(s)$ bandwidth is about 35 Hz, comfortably exceeding the maximum bandwidth of wrist motions, set at 12 Hz. By

appropriately selecting larger values K_P, the bandwidth of $G_{CL}(s)$ can be further extended, reaching 2.8 kHz. Additionally, a higher K_P is necessary to achieve a unitary steady state gain. The derivate gain K_D is tuned instead to obtain the desired damping ratio. The impedance $Z(s)$ remains very low for frequency below the open-loop bandwidth, rising to the value of k_s at a higher frequency.

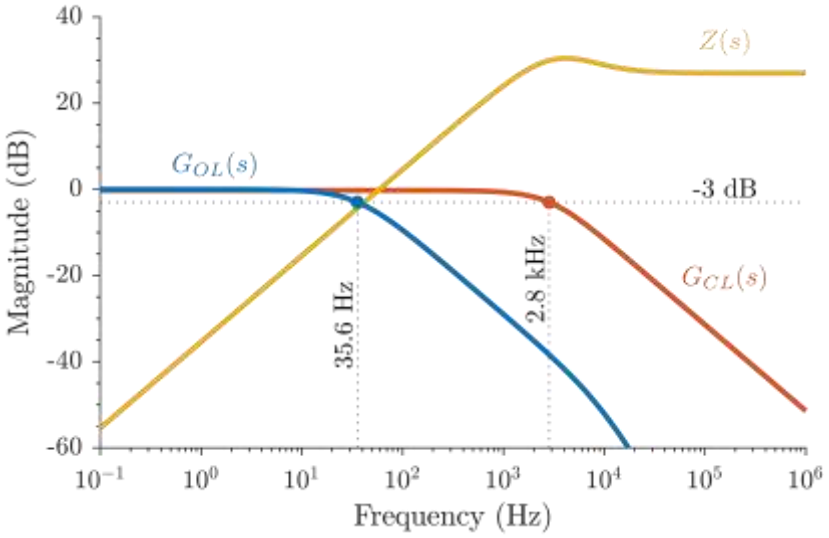

Fig. 5. Frequency responses of the system transfer functions.

These promising results primarily stem from the low estimated inertia J_a, thanks to a design oriented to a lightweight and compact actuation system. Moreover, the hand inertia J_h is relatively low too, resulting in negligible differences in the frequency responses of $G_{CL}(s)$ and $Z(s)$ when considering J_h.

3 Prototype

The proposed final design of the actuator is shown in Fig.6. To obtain the lightest design possible, most of the parts will be fabricated in nylon using additive manufacturing. The expected weight of the system should be approximately 100 g, occupying a volume of $96\ mm \times 51\ mm \times 30\ mm$. The additive manufacturing approach is also exploited to make the cycloidal outer ring of the second stage and the pulley driving the two tendons as one part to maximize the compactness of the transmission.

PTFE pneumatic tubing is used for Bowden cable sheathing, paired with a nylon fishing line for the cable itself. This solution should minimize the friction losses in the cables. Using pneumatic tubing also allows using pneumatic fittings to quickly mount the Bowden cable sheathing.

An earlier version of the cycloidal drive was fabricated in nylon and assembled to assess the feasibility of the design and proved to be a promising solution.

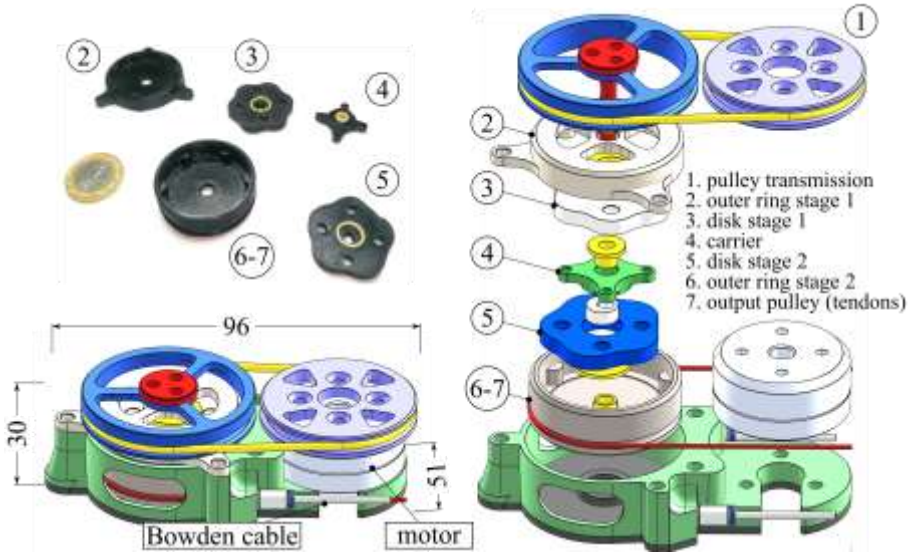

Fig. 6. Final design of the proposed actuator subsystem. On the top left, there is the unassembled 3D-printed cycloidal drive.

Subsequent design iterations will focus on the elastic element, exploring custom torsion spring design possibilities or the utilization of commercial springs (linear or torsional) arranged to achieve the desired equivalent stiffness. The choice between the two alternatives will be guided by the ability to achieve the requirements while maximizing compactness and minimizing weight. In this sense, monolithic solutions seem the most promising, but at the same time they are not trivial in design [13].

4 Conclusions

This work outlines the preliminary design of a highly compact compliant actuator intended for remote assistance of wrist motions or similar joints within exoskeleton applications. First, a space-optimized actuator featuring a 2-stage cycloidal transmission and a tendon-like transmission is proposed. Later, the compliant element of the SEA actuator is sized to achieve the desired performance. A dynamic model of the whole system drives the design, leading to a possible final design of the proposed actuator.
The forthcoming steps involve the fabrication of a prototype for assessment against modeled dynamics. If deemed promising, integration into the exoskeleton will follow.

5 References

1. WHO - World Health Organization. Global report on health equity for persons with disabilities. World Health Organization (2022).
2. Robinson LS, Brown T, O'Brien L. Capturing the costs of acute hand and wrist injuries: Lessons learnt from a prospective longitudinal burden of injury study. Hand Therapy.;25:119–29. (2020).
3. Hussain S, Jamwal PK, Van Vliet P, Ghayesh MH. State-of-the-Art Robotic Devices for Wrist Rehabilitation: Design and Control Aspects. IEEE Transactions on Human-Machine Systems. 50:361–72 (2020)
4. Vélez-Guerrero MA, Callejas-Cuervo M, Mazzoleni S. Design, Development, and Testing of an Intelligent Wearable Robotic Exoskeleton Prototype for Upper Limb Rehabilitation. Sensors. 2021;21:5411.
5. Laribi MA, Carbone G, Zeghloul S. On the Optimal Design of Cable Driven Parallel Robot with a Prescribed Workspace for Upper Limb Rehabilitation Tasks. J Bionic Eng. 2019;16:503–13.
6. Gonçalves RS, Brito LSF, Moraes LP, Carbone G, Ceccarelli M. A fairly simple mechatronic device for training human wrist motion. International Journal of Advanced Robotic Systems. 17:1729881420974286. (2020).
7. Shi K, Song A, Li Y, Li H, Chen D, Zhu L. A Cable-Driven Three-DOF Wrist Rehabilitation Exoskeleton With Improved Performance. Frontiers in Neurorobotics (2021)
8. Quaglia G, Botta A, Colucci G, Takeda Y. RehaWrist.q - Development of a 3 DoF Cable-Driven End-Effector Wearable Robot for Rehabilitation of the Wrist Joint. In: Petuya V, Quaglia G, Parikyan T, Carbone G, editors. Proceedings of I4SDG Workshop 2023. Cham: Springer Nature Switzerland. p. 136–45 (2023)
9. Botta A, Quaglia G, Takeda Y. Wearable Passive Cable-Driven Wrist Rehabilitation Robot: Design and Preliminary Experiments. In: Okada M, editor. Advances in Mechanism and Machine Science. Cham: Springer Nature Switzerland. p. 103–12 (2023)
10. Neumann DA. Kinesiology of the Musculoskeletal System - Foundations for Rehabilitation. 3rd ed. Elsevier Health Sciences (2016).
11. Yoshii Y, Yuine H, Kazuki O, Tung W, Ishii T. Measurement of wrist flexion and extension torques in different forearm positions. BioMed Eng OnLine;14:115. (2015)
12. Qiao D, Pang GKH, Kit MM, Lam DCC. A new PCB-based low-cost accelerometer for human motion sensing. IEEE International Conference on Automation and Logistics. p. 56–60. (2008)
13. Irmscher C, Woschke E, May E, Daniel C. Design, optimisation and testing of a compact, inexpensive elastic element for series elastic actuators. Medical Engineering & Physics. 52:84–9. (2018)